Preparation and characterization of Lithium-stabilized Colloidal Silica as a silicate densifier for concrete surface treatment

Nguyen Hoang Thien Khoi[1, 2], Nguyen Ngoc Tri Huynh[1,2], Huynh Ngoc Minh[1, 2], Nguyen Khanh Son[1, 2, *]

[1]Faculty of Materials Technology, Ho Chi Minh City University of Technology (HCMUT), 268 Ly Thuong Kiet Street, District 10, Ho Chi Minh City, Viet Nam

[2]Vietnam National University Ho Chi Minh City, Linh Trung Ward, Thu Duc City, Ho Chi Minh City, Viet Nam

[*]Emails: *ksnguyen@hcmut.edu.vn*

Abstract. Enhancing the durability of concrete by safeguarding it against cracking and environmental deterioration is paramount. While silicate-based densifiers have been instrumental in shielding concrete surfaces from wear and environmental factors, the surging popularity of lithium silicate solutions faces a significant impediment due to the high cost of lithium, mainly attributed to its predominant use in manufacturing lithium batteries. To address this substantial challenge, an intriguing approach involves blending lithium silicate with colloidal silica, potentially offering a cost-effective and efficient solution for concrete surface treatment. This study delves into the feasibility of utilizing lithium-stabilized colloidal silica as a silicate densifier, focusing on their preparation, characterization, and efficacy in lab-scale applications. The results demonstrate that lithium-stabilized colloidal silica can heighten surface hardness while concurrently reducing porosity. However, it is worth noting that this approach presents particular challenges, particularly regarding preparation and water resistance, when compared to surfaces treated solely with lithium silicate. Addressing these hurdles holds promise for optimizing and enhancing lithium-stabilized colloidal silica and advancing the concrete surface treatment field in future research endeavours.

Keywords: silicate-based densifier, concrete hardener, lithium silicate hardener, colloidal silica, surface treatment

Classification numbers: 2.9.2, 2.5.3.

1. INTRODUCTION

Concrete is ubiquitous in civil engineering due to its high strength, durability, and affordability. Despite its durability, concrete can be vulnerable to cracking and deterioration over time, ultimately impacting its overall structural integrity and appearance. These issues are primarily caused by phenomena inherent in the hydration and hardening process of Portland

cement, the most crucial concrete component. As the cement hydrates, it undergoes a series of chemical reactions that produce heat and cause the mixture to harden and set. Nonetheless, the concrete may experience internal stresses during the drying and contracting stage, potentially causing shrinkage and cracking. Furthermore, suppose the concrete is subjected to early-age load bearing during construction or transportation. In that case, it can experience additional stresses contributing to cracking and deterioration over time. While some measures can be taken to mitigate these issues, such as reducing the water-cement ratio or adding reinforcement, they must be partially avoided.

The consequences of concrete cracking and deterioration can be significant, especially when the material is exposed to harsh environments such as freeze-thaw cycles, moisture, and chemical attacks. The cracks can become pathways for water and other aggressive agents to penetrate the concrete matrix, leading to more severe deterioration, such as reinforcement corrosion, loss of strength and stiffness, and spalling of the concrete surface [1]. Repair and maintenance of damaged concrete can be costly and time-consuming, often requiring extensive excavation, replacement, or structure strengthening. Therefore, there is a need to develop effective solutions to prevent or mitigate the damage caused by concrete cracking and deterioration, such as various surface treatments, including silicate densifiers.

Silicate-based densifiers have emerged as an alternative to polymer-based coatings for protecting concrete surfaces against environmental factors and wear [2]. These densifiers penetrate the concrete surface and chemically react with free lime to form a denser and more durable material, improving the concrete's strength, abrasion resistance, and overall performance [3]. The ion exchange reaction between the silicate solution $R_2O.SiO_2$ (where R is an alkaline ion, such as Na^+, K^+, or Li^+) and $Ca(OH)_2$ can be summarized as follows [4]:

$$R_2O.SiO_2 + Ca(OH)_2 + yH_2O \rightarrow xCaO.SiO_2.zH_2O + 2ROH + (x + y - x - 1)H_2O \qquad (1)$$
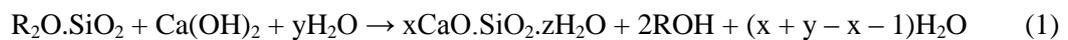
The main product of the reaction is $xCaO.SiO_2.zH_2O$ (C-S-H) is the same mineral formed during cement hydration.

Lithium silicate (LiSi), a chemical compound produced through the fusion of lithium metal and silicate, exhibits considerable promise as an industrial material. It possesses remarkable properties such as abrasion resistance, waterproofing abilities, self-drying characteristics, fire resistance, resilience against adverse weather conditions, and non-toxicity. Due to its compatibility with reduced storage and usage requirements, LiSi has found extensive applications across various industries, including machinery manufacturing, maritime operations, ceramics production, and construction materials [5, 6]. Notably, this material has also made its way into the domain of road transportation. Innovatively, Gransberg and colleagues introduced a lithium-based hardening agent for concrete surface maintenance [7]. Their research unveiled that post-sandblasting treatment effectively mitigated wear and stripe marks, preserving slip resistance on road surfaces for up to three years. Subsequent investigations evaluated the abrasion resistance and gloss retention of limestone treated with lithium silicate, utilizing the AIMS system and Micro-Deval abrasion tests. The results demonstrated that chemical treatment bolstered the hardness and durability of fine particles while upholding angle and gloss resistance under abrasive conditions [8, 9]. Of particular note, the concurrent application of a LiSi hardener with sandblasting yielded intriguing outcomes. Sandblasting improved road surface porosity, enabling deeper penetration of the hardener, resulting in a tougher, more abrasion-resistant surface. Applying a LiSi hardener also maintained the structural integrity and form of the treated surface coating [10]. In summary, the literature above survey underscores the significant

potential of LiSi in enhancing the abrasion resistance of limestone particles and improving the slip resistance of asphalt road surfaces. These benefits can be attributed to the outstanding properties of the resultant robust coating layer, characterized by superior abrasion resistance, waterproofing capabilities, self-drying attributes, and water insolubility. However, the widespread use of LiSi is constrained by the high cost of lithium, primarily due to its priority use in producing lithium batteries.

Developing colloidal silica or nano-silica (CoSi) has opened up new possibilities for concrete surface treatment. Bani Ardalan and colleagues conducted a study to investigate the effects of CoSi particles on concrete's permeability and abrasion resistance by immersing concrete in a diluted CoSi solution. The results showed that maintaining concrete in a CoSi adhesive solution resulted in lower permeability than in regular water [11]. In other words, CoSi hardening reduces the water permeability of concrete. Additionally, the study also indicated that different ratios of CoSi did not significantly affect the permeability of concrete [11]. Pengkun Hou and colleagues also studied the effectiveness and mechanisms of CoSi (with an average particle size of 10 nm) and its precursor, tetraethoxysilane (TEOS), in treating the surface of one-month-old cement mortar samples using brushing techniques [12]. The research showed that CoSi effectively reduced the water absorption ratio of cement mortar when sealed (with adhesive tape) at 50 °C. However, its effect at 20 °C was negligible, especially when maintained under unsealed conditions [12]. Pengkun Hou also studied CoSi and TEOS in the surface treatment of cement concrete, and the results demonstrated that CoSi and TEOS were effective in reducing water absorption and the water vapor transmission properties of concrete, especially in mixtures with a high water/cement ratio [12]. However, the main drawback of nano silica is its stability and ease of use on the construction site [13 - 15].

Combining a mixture of LiSi and CoSi could provide an effective and affordable solution for concrete surface treatment, leading to improved stability, enhanced performance, and increased versatility. This paper investigates the potential use of lithium-stabilized colloidal silica (LSCS) as a silicate densifier for concrete, focusing on their preparation, characterization, and effectiveness in laboratory conditions. In conclusion, a thorough analysis of the benefits and drawbacks of utilizing these materials has been presented, along with the hurdles and prospects that exist in their potential as cost-efficient and efficient concrete surface treatments.

2. MATERIALS AND EXPERIMENTS

2.1. Materials

The LiSi used in our experiments was obtained from Simalco (Belgium) as a commercial product. It has a silicate modulus ranging from 3.5 to 4.8 and possesses desirable characteristics such as transparency and low viscosity. During the experiment of drying the solution in a laboratory oven at 60 °C until it reached a constant weight, it was observed that the solid component content was determined to be 24.63 %. Additionally, the pH of the solution was found to be 12.72 ± 0.01. This high alkaline property is considered an advantage of lithium-based hardeners over those based on sodium and potassium.

Colloidal silica, on the other hand, is a commercially available product from Allied High Tech Product that comprises a suspension of nano-sized silica particles with dispersants. Unlike LiSi, CoSi has an opaque white color and lower viscosity. The solid fraction content in the solution was measured to be 54.17 %, and the pH was recorded as 9.60 ± 0.01. This pH value indicates that the LiSi solution is more alkaline than the CoSi solution. According to literature

studies, it is essential to maintain a pH range of 9 - 11 when working with silica to keep it in a stable colloidal state [16, 17]. This is valuable knowledge to keep in mind for any project involving silica to ensure success.

2.2. Preparation of LSCS solution

The LiSi solution was diluted with distilled water in a 1:1 weight ratio to create the mixture with CoSi. The solution was then stirred for an hour at room temperature using a magnetic stirrer. Subsequently, the CoSi solution was introduced to the diluted LiSi solution with varying weight ratios. It was gradually added while continuous stirring at around 1500 rpm and at a temperature of 50 °C. Figure 1 illustrates some critical steps in the process. As a result, different SiO_2 content in the prepared mixture solutions was achieved, ranging from 0.6 wt% to 10 wt% (Figure 2).
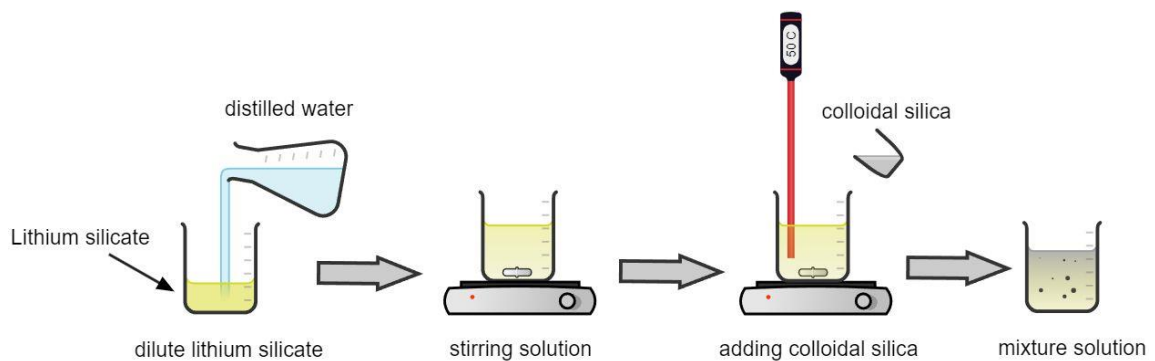
Figure 1. The main steps in processes of a LSCS synthesis.
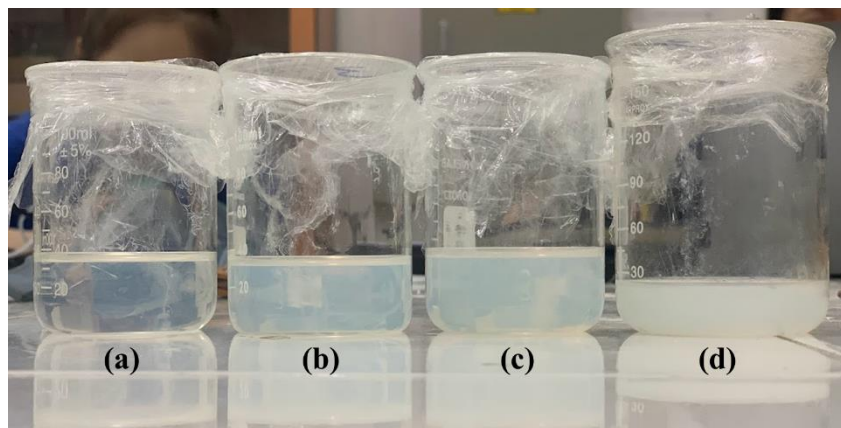
Figure 2. Prepared solution of LSCS with different weight ratios
of SiO_2 (a) 0.6 wt%, (b) 3 wt%, (c) 5 wt% and (d) 10 wt%.

To ensure the stability of the CoSi material and prevent any adverse effects from exposure to air, the beaker container was covered during the 3 hours of stirring time. Following the process, the resulting solution exhibited an opaque white appearance, with the opacity varying depending on the silica content added. The solution was then stored in a sealed beaker for further material analysis and its subsequent use in coating concrete substrates. It is worth noting that these solutions demonstrated excellent stability and homogeneity, remaining unchanged even

after several months of storage at room temperature. However, when the silica content in the mixed solution exceeds 5 wt%, it may lead to instability and result in a milk-white appearance, potentially affecting the aesthetic aspect of the coating solution.

2.3. Preparation of concrete surface and coating experiment

In order to ready the concrete substrate for surface coating, the raw materials were meticulously blended to form cylindrical specimens with a diameter of 11.4 cm and a height of 20 cm. The specimens were composed of 400 ± 2 g Portland cement, 600 ± 5 g river sand as fine aggregate, 520 ± 5 g crushed stone as coarse aggregate with a particle size of sieve 2.5/5, and 225 ± 1 g tap water. After 28 days of curing, the specimens were cut into round discs with a thickness of 15 mm. These discs were then meticulously ground in four consecutive steps using sandpaper (A180, P400, P800, P1000) attached to a hand-held grinding machine. This process aimed to ensure a flat and defect-free surface of the concrete substrate, promoting even coverage of the entire surface and resulting in an aesthetically pleasing appearance after coating.

Figure 3 shows the surface differences in the cement-concrete samples before and after the grinding and washing process. It is apparent that the surface is flatter, and the number of surface defects has significantly decreased compared to the sample before grinding. However, it is worth noting that the surface's dark areas, consisting of sand and stone aggregates, tend to be denser and less permeable to water than the surrounding cement mortar.

The next step involved the application of the soft brush coating method onto the concrete substrate. The surface of the disc sample was divided into four regions, as illustrated in Figure 4, for easy evaluation and comparison between different areas. The coating was consistently applied in two uniform layers, with the second layer being applied after the first had thoroughly dried to maintain homogeneity throughout the test.
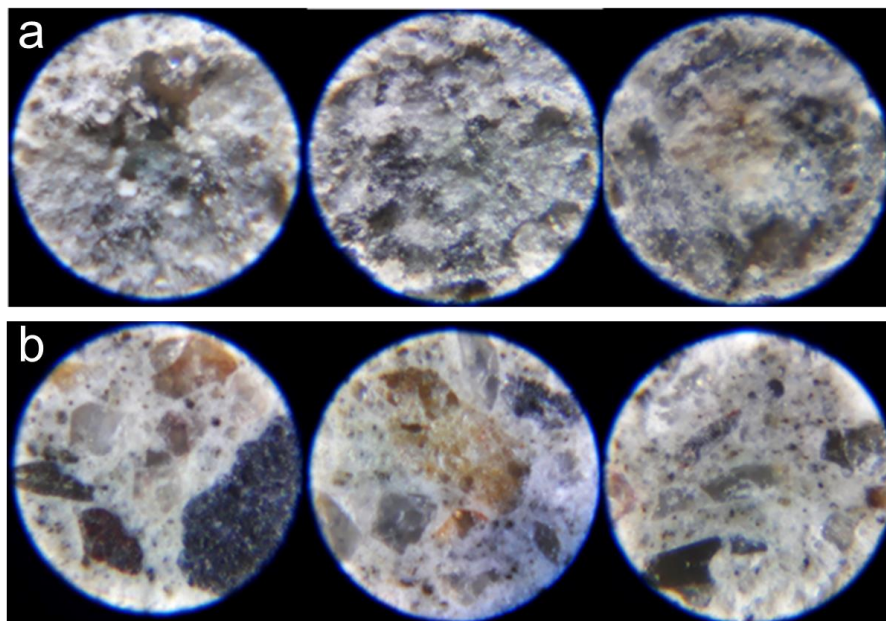
Figure 3. Optical microscope images (x250) of the sample surface before (a) and after (b) grinding process.
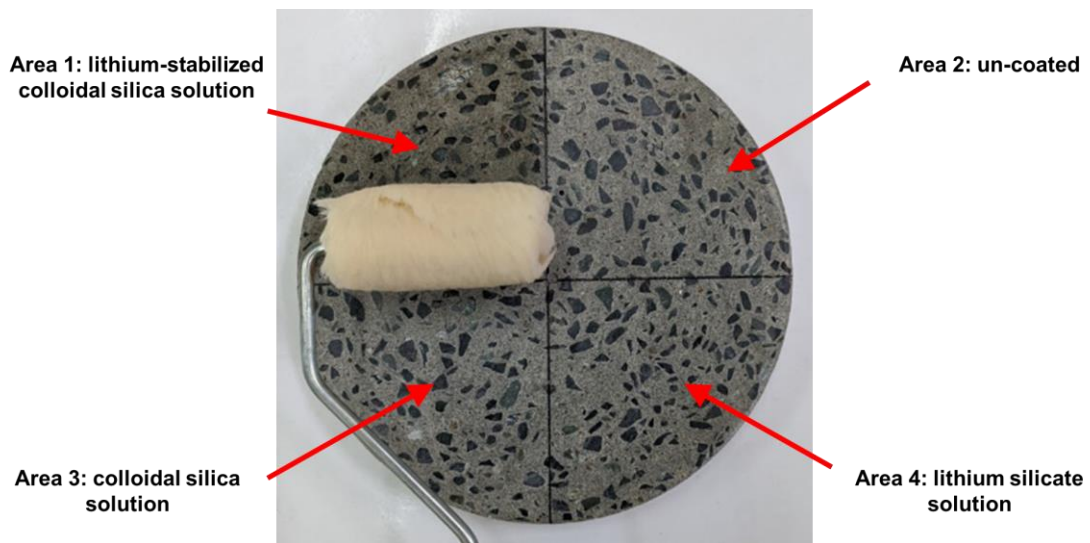
Figure 4. The concrete sample coated with three different silicate densifiers.

2.4. Characterization and test method

This study analyzed the prepared solutions' Fourier Transform Infrared (FTIR) spectra within the wavenumber range of 400 to 4000 cm^{-1}. This analysis used a reflection technique on a NICOLET 6700 FT-IR Spectrometer manufactured by Thermo Fisher Scientific, USA. The primary objective was to examine the chemical characteristics of the prepared solutions. To assess particle size and the stability of particle dispersion within the coating solution, an LSCS solution with a silica content of 10 wt% underwent analysis. This analysis included determining particle size distribution using Dynamic Light Scattering (DLS) and zeta-potential testing, performed using the Horiba SZ-100V2 Instrument.

Furthermore, the study emphasized the analysis of coating morphology and microstructure. For this purpose, an optical microscope, specifically the Kyowa Me-Lux-3 model, and a scanning electron microscope (SEM), specifically the Hitachi S-4800 model, were employed. These instruments facilitated the examination of the physical characteristics and structure of the coatings. After a designated period for the coating to react with the substrate, various tests were conducted to evaluate the coated surface. These tests included assessments of water absorption and Mohr hardness. To evaluate water absorption characteristics, pedestal samples treated with various coating solutions (as mentioned previously) underwent a meticulous evaluation process. After a curing period of 7 days, the samples were hermetically sealed along their bases and surrounding areas using a uniform layer of aluminum adhesive. This sealing process ensured a consistent coating thickness. Subsequently, the sealed samples were immersed in water, with the water level precisely reaching half the thickness of the pedestal sample. This immersion brought the coated surface into direct contact with the aqueous medium. The samples were carefully extracted and promptly fractured at specific intervals of 1-, 2-, and 3-hours following immersion. This fracture facilitated observations of the extent of water ingress into the thickness of each coating region. It is important to note that the fracture point was consistently situated at the central region of the coated area. This deliberate choice was made to minimize potential variations in water penetration that might arise from different coating regions on the same pedestal sample.

The evaluation of surface scratch resistance for concrete samples reinforced with a strengthening layer followed the prescribed methodology outlined in ASTM C1895 – 20. The assessment was carried out using the Mohs hardness testing method. Each area with a coating layer was firmly affixed to a robust support structure. A Mohs hardness pen, positioned at a precise 70-degree angle, was utilized to induce scratches on the surface of the concrete sample. The pointed tip of the Mohs hardness pen was employed for this purpose. The material scratching during this process indicated that the material's hardness was lower than the value indicated on the hardness pen. The testing procedure continued systematically, utilizing a series of pens with progressively lower hardness values. This process was repeated until the material showed no signs of scratching. The cessation of scratching served as the point of reference for accurately determining the hardness level of the applied coating layer. This standardized method, by ASTM C1895 – 20, provided a reliable means to assess and quantify the scratch resistance of the concrete samples with their strengthening layers.

3. RESULTS AND DISCUSSION

3.1. Characterization of prepared solution of LSCS

Figure 5 displays the FTIR spectra of LiSi, CoSi, and four mixture solutions of LSCS (with different silica content) in the wavelength range of 4000-400 cm^{-1}. The infrared spectrum of the LiSi solution reveals the presence of free H-O-H and O-H bonding in the range of 3650 to 3150 cm^{-1}, along with H-O-H bonds at 1638 cm^{-1}[18]. The 1037 cm^{-1} and 445 cm^{-1} peaks correspond to Si-O-Si oscillation [19, 20]. The characteristic Si=-O bond is also observed at a wave number of 1196 cm^{-1} [21]. In the infrared spectrum of the CoSi solution, the asymmetric stretching and shear bands of the Si–O–Si bonds are seen at 1093 cm^{-1}, while the symmetrical stretching vibrations of the Si=O bonds and the bending vibrations of the Si–O–Si bonds are observed at 801 and 469 cm^{-1}, respectively [21]. Moreover, a broad, intense absorption peak at 3420 cm^{-1} corresponds to the adsorbed water molecules [18].

The infrared spectra of the mixture solutions with silica content ranging from 0.6 wt% to 10 wt% show common peak positions in the range of 3650 to 3150 cm-1, which are characterized by the H-O-H and free O-H bonds, along with the appearance of the H-O-H bond at 1638.0 cm^{-1} [18]. The Si-O-Si bond appears at around 1037 cm^{-1} in all spectrums [21]. Additionally, the Si=O bond appears at 773.3 cm^{-1}, and the Si-O-Si bond appears at 445 cm^{-1} [21].
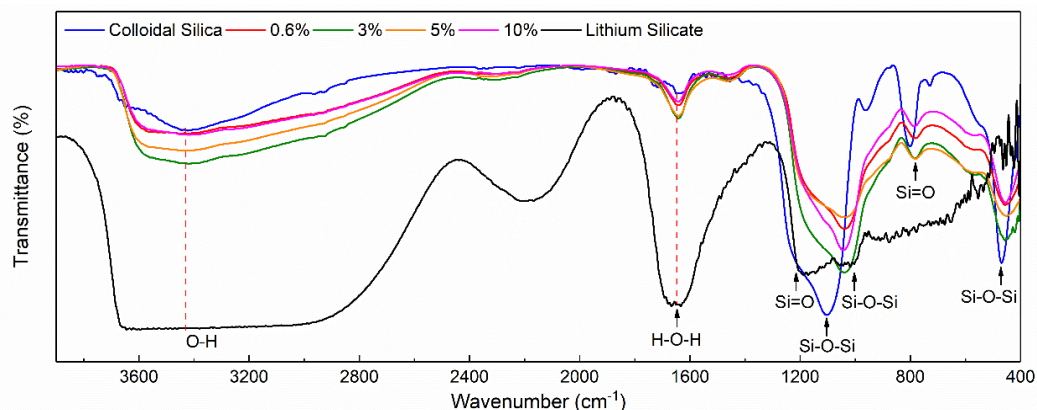
Figure 5. FTIR spectra of various concrete densifiers including: LiSi solution, CoSi and prepared solution of LSCS.

Based on the FTIR analysis results, it can be inferred that the mixture of CoSi and LiSi exhibits characteristic peaks such as Si-O-Si and H-O-H bonds. The mixing process of the two solutions does not indicate the appearance of new bonds, and the solution is homogeneous with good dispersion of the components. The obtained spectra demonstrate an average transmission of the mixed spectra of the two raw components, reflecting the mixture ratio.
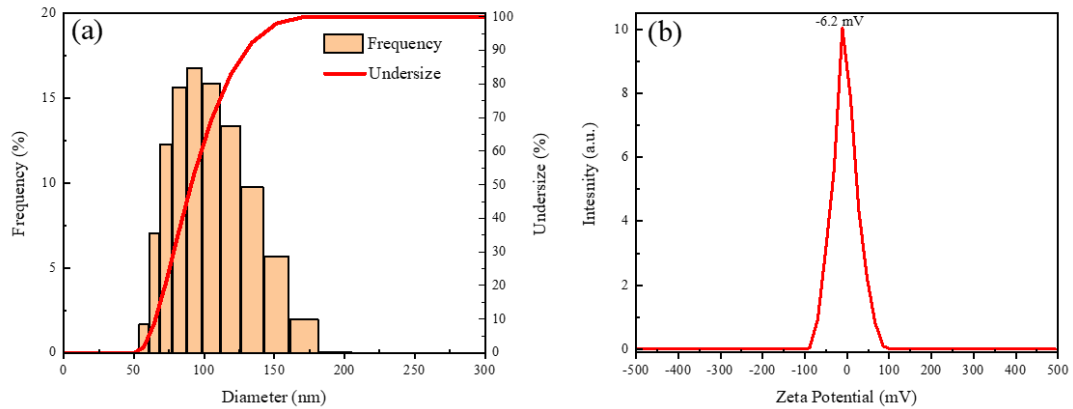
Figure 6. (a) Particle size distribution result; (b) Pattern of zeta potential of the solution of LSCS with 10 wt% silica.

Figure 6 depicts the particle size distribution of a LSCS solution containing 10 wt% silica contents. The analysis results indicate that the particle sizes range from 50.53 nm to 193.48 nm, with an average particle size of 88.6 nm. This average size slightly increases compared to the average particle size of the CoSi material, typically 75 nm. However, the size distribution spectrum overall exhibits good concentration (Figure 6-a). The increase in silica particle size at the nanoscale may be attributed to emulsion flocculation. Agglomeration is a common phenomenon observed in colloidal solutions, where small particles come into contact and adhere to one another, forming larger clusters. Agglomeration can be influenced by particle concentration, pH, temperature, and stabilizing agents [22, 23].

Additionally, the zeta surface potential measurement method was employed to investigate the stability of the emulsion solution. The zeta potential pattern of the solution sample displays a peak potential at -6.2 mV (Figure 6-b). Comparing this value to the range of potential values associated with solution stability, it can be concluded that the synthesized solution exhibits relatively stable characteristics. This observation aligns with the visual assessment of the solution, as shown in Figure 2.

3.2. Precipitation reaction between silicate densifier solutions and Ca(OH)$_2$

Figure 7 illustrates the experimental process of monitoring the reaction between the coating solutions and Ca(OH)$_2$. The results showed that adding LiSi to Ca(OH)$_2$ resulted in the formation of a white precipitate at room temperature, which increased in amount over time at 1 day, 3 days, and 7 days. This suggests that the reaction between LiSi and Ca(OH)$_2$ was ongoing and that the precipitate continued to form as time progressed and the presence of a high concentration of Ca^{2+}.

| | Start | Day 1 | Day 3 | Day 7 |

Lithium silicate

Lithium-stabilized colloidal silica

Colloidal silica solution
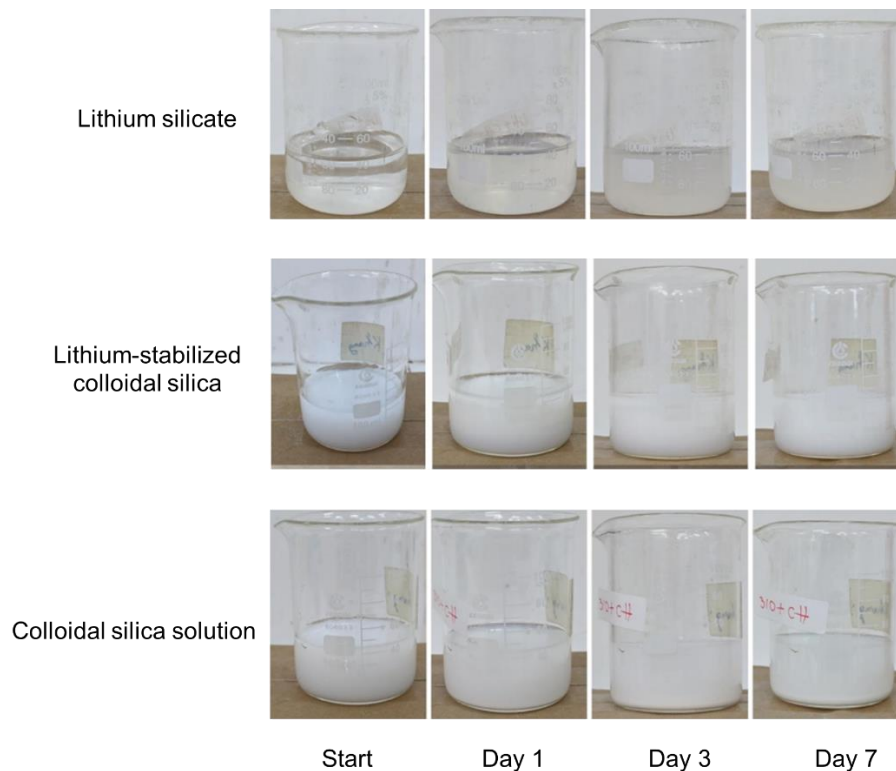
Figure 7. Monitoring the progress of precipitation reaction between silicate densifier solutions and $Ca(OH)_2$.

In contrast, adding $Ca(OH)_2$ to the CoSi solution caused the immediate destabilization of the CoSi solution, leading to agglomeration and settling of nano-silica particles to the bottom of the beaker. The settled precipitate made it challenging to observe the amount formed accurately. However, gradually clarifying the solution above the settled portion was observed over time. This hindered the ability to determine the appropriate amount of CoSi for the reaction, posing difficulties in the application process. The loss of stability of CoSi when added to the $Ca(OH)_2$ solution is in line with previous research, where the ion composition and concentration of the surrounding environment of the nano-silica particles cause instability of the CoSi solution [24]. The presence of one-valence and two-valence ions, such as calcium (Ca^{2+}), changes the ion charge of the silica sol and leads to two agglomeration mechanisms. The first mechanism reduces the electrostatic repulsion force between the nano silica particles, making the attractive force dominant. Additionally, these ions can bridge between the nano-silica particles, neutralizing positions on the silica surface and forming physical bridges between two silica particles if their charge-neutral surfaces collide and coordinate with the water oxygens binding to the surfaces [24].

In the prepared solution of LSCS, it was observed that initially, a white precipitate formed and later settled. This phenomenon can be attributed to the high pH of the $Ca(OH)_2$ solution, which disturbs the non-agglomeration equilibrium of the synthesis solution. However, it is important to note that when the solution is applied as a coating on cement-concrete substrates, the concentration of $Ca(OH)_2$ available is significantly lower compared to the test conditions of the solution. Consequently, the formation of precipitated minerals through the combination

reaction process may occur gradually over time, in contrast to the initial agglomeration and settling state of the CoSi.
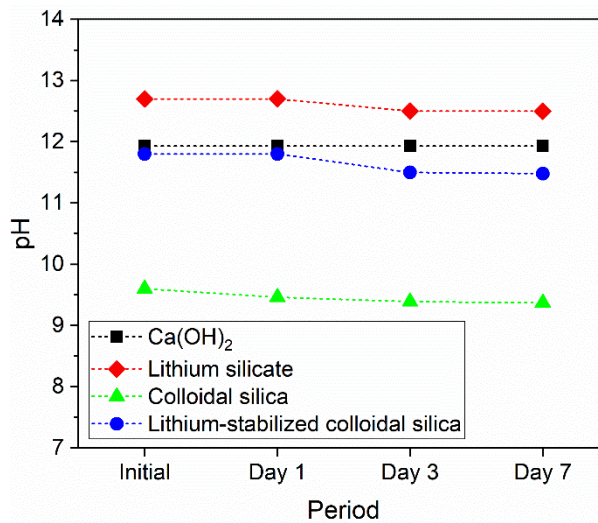
Figure 8. pH values of reaction solutions with $Ca(OH)_2$ at 1 day, 3 days, and 7 days intervals.

In this study, the reactivity of a $Ca(OH)_2$ solution with various silicate solutions was rigorously investigated by monitoring pH values within reaction samples over three distinct time intervals: one day, three days, and seven days. The objective was to understand how these solutions interacted chemically and how their pH levels evolved. Upon conducting a one-day observation, it was observed that the pH values of the LiSi and CoSi solutions exhibited a slight decrease. This initial change in pH suggested the formation of acidic products resulting from the reactions. However, the pH value of the LSCS solution remained notably stable at approximately 11.83 during this brief timeframe, indicating that this particular solution did not yield acidic products within the early stages of the reaction.

As the reaction proceeded over three days, a consistent trend emerged. The pH values of all solutions continued to decline, indicating an ongoing chemical transformation. Specifically, the pH values of the LiSi and CoSi solutions decreased further to 10.05 and 10.39, respectively. This decline indicated a more pronounced formation of acidic products resulting from the interactions between these silicate solutions and $Ca(OH)_2$. Interestingly, the pH value of the LSCS solution showed a relatively minor decrease to 11.50, maintaining a higher pH compared to the other two solutions. Extending the reaction period to seven days further intensified the downward trend in pH values for all solutions. The pH values of the LiSi and CoSi solutions decreased to 10.01 and 10.37, respectively, underscoring the continuous formation of acidic products. In contrast, the pH value of the LSCS solution remained almost stable, with only a slight decrease to 11.48. These findings explain the chemical reactivity between $Ca(OH)_2$ and different silicate solutions. The pH of all three densifier solutions decreased compared to the initial $Ca(OH)_2$ solution, signifying a reduction in the alkalinity of the solutions due to the ongoing reactions. Notably, the extent of pH reduction varied among the different silicate solutions, with the reaction between LiSi and $Ca(OH)_2$ leading to a more pronounced reduction in pH, consistent with the formation of acidic products. In contrast, the reaction between CoSi and $Ca(OH)_2$ resulted in a pH decrease compared to the initial $Ca(OH)_2$ solution. However, it maintained a pH level higher than the original CoSi solution, suggesting that the reaction product had a pH-altering effect that was less

acidic than the reaction involving LiSi and $Ca(OH)_2$. These findings contribute to understanding the complex chemical interactions between these solutions and their evolving pH dynamics over time.

The higher pH value observed in the LSCS solution compared to the LiSi and CoSi solutions can be elucidated by the stabilizing influence of lithium ions on CoSi particles [25]. CoSi particles inherently possess a high surface area and a propensity to undergo aggregation, leading to instability and a concurrent decrease in pH value. However, introducing lithium ions into the LSCS solution is pivotal in mitigating this aggregation phenomenon. Lithium ions exhibit a capacity to interact with the surface of CoSi particles, forming a protective layer that acts as a barrier against aggregation. This protective layer maintains the stability of the CoSi solution [25]. As a result, the LSCS solution exhibits a higher pH value than the LiSi and CoSi solutions, both lacking this stabilizing effect [25]. Therefore, the elevated pH value observed in the LSCS solution can be primarily attributed to lithium ions, which contribute significantly to stabilizing CoSi particles. This stabilization effect is crucial in maintaining the solution's pH level and preventing the formation of acidic products, as observed in the experimental results.

3.3. Characterization of coated concrete sample

3.3.1. Visualization by optical microscope

The optical microscope images in Figure 9 provide a detailed view of the surface morphology of different coating layers on the sample. By comparing the uncoated and coated samples, it can be observed that the coating layers effectively filled the surface defects, such as pores and cracks, resulting in a smoother surface. This could be attributed to the materials in the coating layer that could penetrate and fill in the pores and cracks, leading to a more uniform surface.

The color variation among the coating layers is also significant. The transparency of the LiSi coating layer implies that it is a suitable coating for preserving the original color and texture of the coated material. In contrast, the milky white color of the CoSi coating layer suggests the presence of nano-silica particles in the coating. The color of the LSCS coating layer is less milky white than the CoSi coating layer, indicating that the LSCS solution may be a better option for achieving a more natural appearance. The adhesion of the coating layer on the surface is also a crucial aspect to consider. The LiSi and LSCS coating layers exhibited adhesion on the aggregate positions' top surface, suggesting that these coatings are better suited for protecting and preserving the aggregate areas. On the other hand, the CoSi coating layer covered the entire surface of the aggregate and cement mortar positions. However, it formed non-continuous scales that overlapped, potentially resulting in weaker adhesion and less protection for the aggregate areas. The smaller and less dense scales observed in the LSCS coating layer indicate that it may provide better protection and adhesion than the CoSi coating layer.

3.3.2. Morphological analysis by SEM

Figure 10 depicts scanning electron microscopy (SEM) images of the surface areas coated with LiSi, CoSi, and LSCS solutions. The uncoated concrete surface exhibited a typical microstructure with loosely arranged C-S-H minerals, resulting in visible pores. This porosity increases the risk of material corrosion and degradation, emphasizing the need for a protective coating.
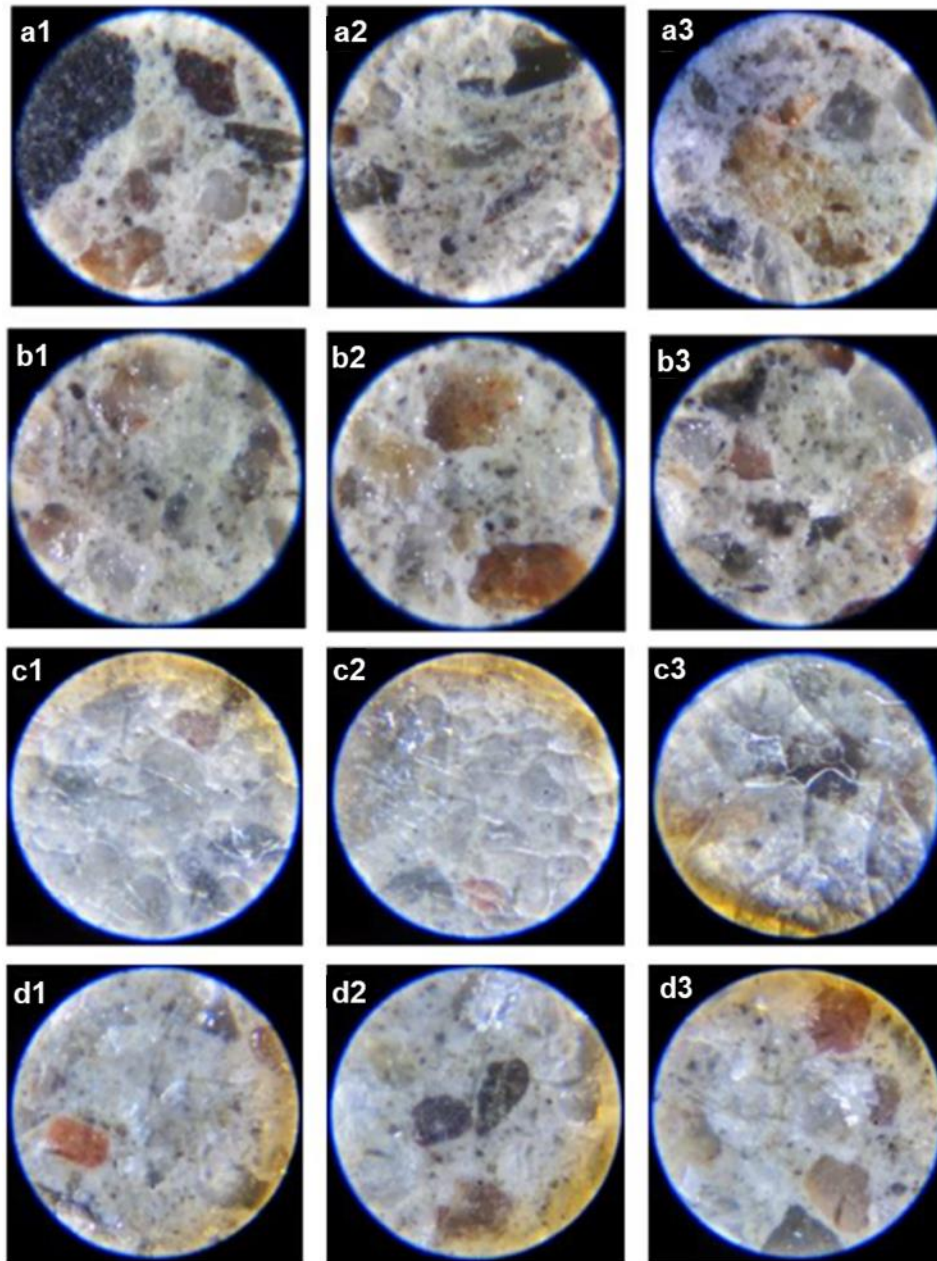
Figure 9. Optical microscope images (x250) of the sample surface of (a1) – (a3) uncoating area, (b1) – (b3) area coated with LiSi, (c1) – (c3) area coated with CoSi, and (d1) – (d3) area coated with LSCS (d) after 14 days.

The surface coated with LiSi solution displayed a continuous background that filled the pores and resulted in a denser and more continuous surface. This suggests that the coating solution reacted with the concrete, forming a strong bond and changing the microstructure of the surface. The density of the C-S-H mineral also increased significantly, indicating that the coating solution effectively stiffens and strengthens the surface. Observations at higher magnifications revealed the formation of rod-shaped C-S-H minerals on the concrete background after 14 days

of coating with the LiSi solution. This indicates that the coating solution promotes the growth of C-S-H minerals known to improve the strength and durability of concrete. $Ca(OH)_2$ minerals were also observed on the concrete background surface in the shape of hexagonal plates, and it is predicted that they react with the coating solution to form a strong bond, enhancing the performance of the coating layer. The LSCS coating was also effective in improving the microstructure of the concrete surface, with thin rod-like C-S-H minerals observed in the void spaces. The CoSi coated area also exhibited uneven surface morphology. However, it showed the presence of C-S-H and $Ca(OH)_2$ minerals, suggesting that the coating solution reacted with the concrete and formed a strong bond.
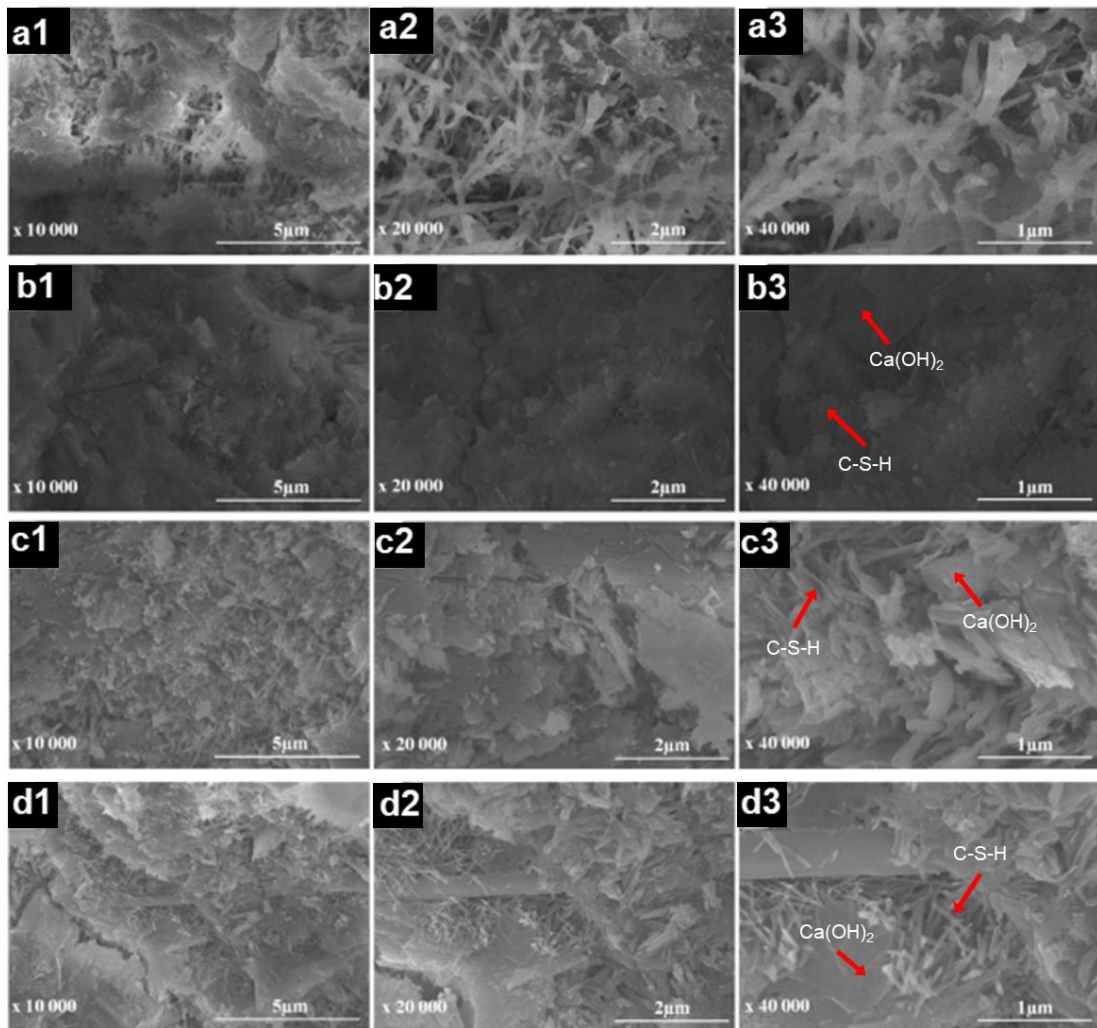
Figure 10. SEM images of the sample surface of (a1) – (a3) uncoating area, (b1) – (b3) area coated with LiSi, (c1) – (c3) area coated with CoSi, and (d1) – (d3) area coated with LSCS after 14 days.

Overall, the coated sample surfaces showed higher compactness than the uncoated sample, indicating that a product layer was deposited on the surface, altering the microstructure of the concrete surface. The presence of $Ca(OH)_2$ minerals was also observed, and it is predicted that

the reaction between the coating layer and Ca(OH)$_2$ will continue over time under favorable conditions (temperature, humidity). These findings demonstrate the effectiveness of the coating solutions in improving the durability and performance of concrete structures.

3.3.3. Water absorption

Figure 11 depicts the depth of water penetration through various sample areas at 1, 2, and 3 hours after immersion. Upon immersion of the concrete sample in water for 1 hour, it was observed that water had penetrated all areas of the sample, including the areas coated with the LSCS, CoSi, and LiSi solutions, as well as the uncovered areas. The thickness of water penetration in the uncovered area was significantly higher than that of the coated areas, indicating that the water resistance of the coated areas was superior under the same experimental conditions. The consistency of the results obtained from points equidistant from the sample surface in contact with water further validated the reliability of the findings.
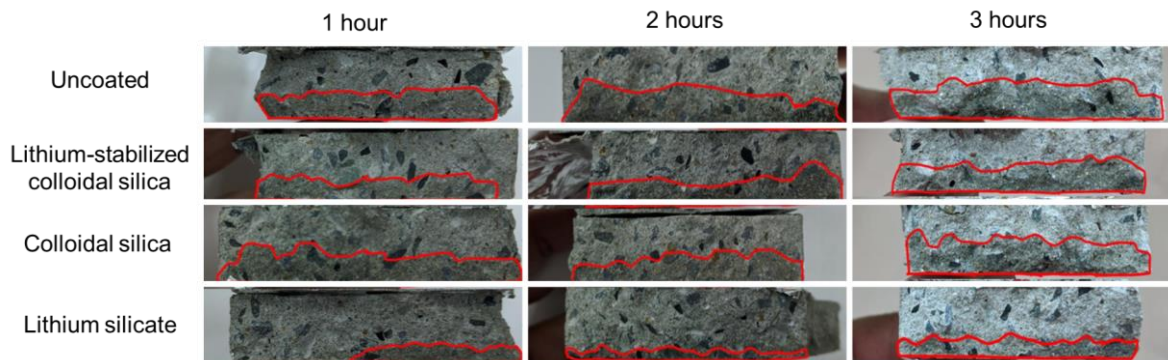
Figure 11. Water absorption rate through different sample areas at time intervals of 1, 2, and 3 hours after immersion.

Subsequent immersion of the sample for 2 and 3 hours and examination of the results upon breaking the samples showed that the thickness of water penetration in the areas coated with the LSCS solution did not differ significantly from that of the areas coated with the CoSi solution. However, the thickness of water penetration in the areas coated with LiSi solution was lower than in the other areas, indicating that the surface water resistance of the sample coated with LiSi solution was better than that of the LSCS and CoSi. This suggests that LiSi has superior permeability and reaction compared to CoSi. Additionally, analysis of Figure 9 revealed that the coating layer on the surfaces covered with CoSi and the LSCS solution had a flaky form. In contrast, the coating layer of LiSi formed a continuous layer. This difference in coating layer structure may have contributed to the variance in water penetration ability observed in the different sample areas.

3.3.4. Scratch resistance (Mohs hardness)

Table 1 presents the results of the surface hardness measurements of concrete samples coated with three solutions: LiSi, CoSi, and LSCS, as measured by the Mohs scale after 14 and 21 days of coating. Using a Mohs pen allowed the hardness of the samples at various positions to be measured, thereby evaluating the effect of the testing pen on the coating layer. The

presented hardness values indicate the relative hardness between different coated areas, which provides insight into the effectiveness of the coating layer on the concrete surface over time.

The results reveal that after 7 days, the surface hardness of the LSCS and LiSi coated areas were the same, with a hardness level 5.5. In contrast, the surface hardness of the CoSi coated area was only 3.5. After 21 days, the surface hardness of the LiSi coated areas increased to 6.5, while the surface hardness of the LSCS solution coated area was 6. The surface hardness of the CoSi coated area at 21 days was 4. These findings suggest that the surface hardness of the concrete samples increases from 7 to 21 days, indicative of a combination reaction and increased surface density. However, significant hardness differences between the coating solutions indicated variations in their effectiveness. Specifically, the surface hardness of the CoSi coated area was lower than that of the LiSi and LSCS solution coated areas at 7 and 21 days. This suggests that the reaction ability of the CoSi solution with the concrete sample was suboptimal. Thus, CoSi may be considered a less effective coating solution than LiSi. These results highlight the importance of evaluating coating solutions' performance and efficacy over time.

Table 1. Surface hardness of coatings according to Mohs scale at 14 and 21-day intervals.

Time of reaction	Hardness level in Mohs scale		
	LiSi	*CoSi*	*LSCS*
7-day	5.5	3.5	5.5
21-day	6.5	4.0	6

4. CONCLUSIONS

In conclusion, the experimental results obtained from investigating and assessing a LiSi solution and a mixture comprising CoSi and LiSi (up to 10 wt% silica) have revealed promising attributes. The two-component mixture exhibits a homogeneous composition and well-dispersed components, as evidenced by FTIR analysis and particle size measurements. During its reaction with $Ca(OH)_2$, the LSCS solution precipitates and forms a crystallized product.

Moreover, optical microscope and SEM images illustrate that applying the LSCS solution onto a concrete surface creates a continuous, smooth background that effectively conceals porous regions and cracks. This results in a more polished and lustrous surface when compared to untreated areas. Over 7 and 21 days, the surface hardness of the concrete samples coated with the LSCS gradually increases, indicating a noticeable enhancement in the surface hardness.

Furthermore, the LSCS demonstrates superior water resistance properties to the uncoated concrete surface. However, it is worth noting that the water permeability of the samples coated with LSCS still differs from that of samples coated with pure LiSi.

In light of these findings, the two-component mixture of CoSi and LiSi shows promise as a cost-effective alternative to traditional LiSi solutions for concrete surface treatment. Nonetheless, further research is necessary to optimize its characteristics and effectiveness, ensuring its suitability for various concrete applications.

Credit authorship contribution statement. Author 1: Investigation, Manuscript preparation. Author 2: Formal analysis. Author 3: Formal analysis. Author 4: Manuscript revision, Methodology, Supervision.

Declaration of competing interest. The authors declare that they have no known competing financial interests or personal relationships that could have appeared to influence the work reported in this paper.

REFERENCES

1. Neville A. M., Brooks J. J. - Concrete technology, Longman Scientific & Technical, England, 1987.

2. Pan X., Shi Z., Shi C., Ling T. C., Li N. - A review on concrete surface treatment Part I: Types and mechanisms, Constr. Build. Mater. **132** (2017) 578-590. https://doi.org/ 10.1016/j.conbuildmat.2016.12.025.

3. Kim J., Kitagaki R. - Behavior of hydrates in cement paste reacted with silicate-based impregnant, Cem. Concr. Compos. **114** (2020) 103810. https://doi.org/10.1016/ j.cemconcomp.2020.103810.

4. Provis J. L., Van Deventer J. S. - Alkali activated materials: state-of-the-art report, Springer Science & Business Media, Germany, 2013.

5. Kato Y., Someya N. - Effect of silicate-based surface penetrant on concrete durability, in: Grantham M., Muhammed Basheer P. A., Magee B. and Soutsos M. (Eds.), Concrete Solution, Taylor & Francis Group, London, 2014, pp. 393-397.

6. Hazehara H., Soeda M., Hashimoto S. - Fundamental study on characteristics of silicate based surface penetrants and effects of improvement on concrete structures, in: Furuta H., Frangopol D. and Akiyama M. (Eds.) , Life-Cycle of Structural Systems: Design, Assessment, Maintenance and Management, CRC Press, London, 2014, pp. 971-978.

7. Gransberg D. D., Pittenger D. M. - Maintaining Airport Pavement Friction Using Surface Densification, Proceedings of the 9th International Conference on Managing Pavement Assets, Vol. 9, Washington, 2015, pp. 300-309.

8. Zhang H., Zhang Z., Lv J., Zhang G. - Effect of Lithium Silicate–Impregnated Limestone Aggregate on Skid Resistance Properties of Bituminous Mixture, J. Mater. Civ. Eng. **34** (2022) 04022251. https://doi.org/10.1061/(ASCE)MT.1943-5533.0004409.

9. Zhang Z., Zhang H., Lv J., Li W. - Performance evaluation of skid-resistant surface treatment using lithium silicate for limestone bituminous pavement, Constr. Build. Mater. **342** (2022) 127990. https://doi.org/10.1016/j.conbuildmat.2022.127990.

10. Lv J., Wang R. - Literature Review of Shot Blasting and Lithium Silicate Treatment to Improve the Anti-sliding Performance of Asphalt Pavement, Proceedings of the 5th International Conference on Information Science, Computer Technology and Transportation, Vol. 5, Shenyang, 2020, pp. 662-666.

11. Ardalan R. B., Jamshidi N., Arabameri H., Joshaghani A., Mehrinejad M., Sharafi P. - Enhancing the permeability and abrasion resistance of concrete using colloidal nano-SiO_2 oxide and spraying nanosilicon practices, Constr. Build. Mater. **146** (2017) 128-135. https://doi.org/10.1016/j.conbuildmat.2017.04.078.

12. Hou P., Cheng X., Qian J., Shah S. P. - Effects and mechanisms of surface treatment of hardened cement-based materials with colloidal nanoSiO2 and its precursor, Constr. Build. Mater. **53** (2014) 66-73. https://doi.org/10.1016/j.conbuildmat.2013.11.062.

13. Jalal M., Mansouri E., Sharifipour M., Pouladkhan A. R. - Mechanical, rheological, durability and microstructural properties of high performance self-compacting concrete containing SiO2 micro and nanoparticles, Mater. Des. **34** (2012) 389-400. https://doi.org/10.1016/j.matdes.2011.08.037.

14. Ji T. - Preliminary study on the water permeability and microstructure of concrete incorporating nano-SiO$_2$, Cem. Concr. Res. **35** (2005) 1943-1947. https://doi.org/10.1016/j.cemconres.2005.07.004.

15. Land G., Stephan D. - The influence of nano-silica on the hydration of ordinary Portland cement, J. Mater. Sci. **47** (2012) 1011-1017. https://doi.org/10.1007/s10853-011-5881-1.

16. Gu S., Shi Y., Wang L., Liu W., Song Z. J. C., Science P. - Study on the stability of modified colloidal silica with polymer in aqueous environment, Colloid Polym. Sci. **292** (2014) 267-273. https://doi.org/10.1007/s00396-013-3109-4.

17. Chung I., Kim T., Kang J., Tan M. M., Dung N. T. K., Huynh M. D., Dai Lam T., Chinh N. T., Giang B. L., Hoang T. J. C., Physicochemical S. A., Aspects E. - Preparation, stabilization and characterization of 3-(methacryloyloxy) propyl trimethoxy silane modified colloidal nanosilica particles, Colloids Surf., A **585** (2020) 124066. https://doi.org/10.1016/j.colsurfa.2019.124066.

18. Kloprogge J. - Application of vibrational spectroscopy in clay minerals synthesis, Dev. Clay. Sci. **8** (2017) 222-287. https://doi.org/10.1016/B978-0-08-100355-8.00008-4.

19. Dorosz D., Zmojda J., Kochanowicz M. - Investigation on broadband near-infrared emission in Yb^{3+}/Ho^{3+} co-doped antimony–silicate glass and optical fiber, Opt. Mater. **35** (2013) 2577-2580. https://doi.org/10.1016/j.optmat.2013.07.022.

20. Ivanov V. G., Reyes B. A., Fritsch E., Faulques E. - Vibrational states in opals revisited, J. Phys. Chem. C **115** (2011) 11968-11975. https://doi.org/10.1021/jp2027115.

21. Khan R., Khare P., Baruah B. P., Hazarika A. K., Dey N. C. - Spectroscopic, kinetic studies of polyaniline-flyash composite, Adv. Chem. Engineer. Sci. **1** (2011) 37-44. https://doi:10.4236/aces.2011.12007.

22. Zeng N., Zhao H., Liu Y., Wang C., Luo C., Wang W., Ma T. - Optimizing of the colloidal dispersity of silica nanoparticle slurries for chemical mechanical polishing, Silicon **14** (2022) 7473–7481. https://doi.org/10.1007/s12633-021-01448-y.

23. Becit B., Duchstein P., Zahn D. - Molecular mechanisms of mesoporous silica formation from colloid solution: Ripening-reactions arrest hollow network structures, PLoS ONE **14** (3) e0212731. https://doi.org/10.1371/journal.pone.0212731.

24. Hendrix D., McKeon J., Wille K. - Behavior of colloidal nanosilica in an ultrahigh performance concrete environment using dynamic light scattering, Materials **12** (2019) 1976. https://doi.org/10.3390/ma12121976

25. da Cruz Schneid A., Albuquerque L. J. C., Mondo G. B., Ceolin M., Picco A. S., Cardoso M. B. - Colloidal stability and degradability of silica nanoparticles in biological fluids: A review, J. Sol-Gel Sci. Technol. **102** (2022) 41-62. https://doi.org/10.1007/s10971-021-05695-8.